



TITLE:

Flow Properties and Fiber Formation of Alumina Sols

AUTHOR(S):

Maki, Toshio; Sakka, Sumio

CITATION:

Maki, Toshio ...[et al]. Flow Properties and Fiber Formation of Alumina Sols. Bulletin of the Institute for Chemical Research, Kyoto University 1988, 65(5-6): 242-251

ISSUE DATE:

1988-03-15

URL:

<http://hdl.handle.net/2433/77204>

RIGHT:

Flow Properties and Fiber Formation of Alumina Sols

Toshio MAKI* and Sumio SAKKA*

Received November 18, 1987

The effects of the Al_2O_3 and Cl^- ion contents on the flow properties of Al_2O_3 sols prepared from inorganic materials have been examined for the sols in which the Al_2O_3 content ranges from 1.9 mol/dm^3 to 3.0 mol/dm^3 and the Cl^- ion content ranges from 0.5 mol/dm^3 to 3.0 mol/dm^3 . It has been found that a sol with less than 0.7 mol/dm^3 Cl^- ion exhibits the thixotropy and that all other sols are characterized with the Newtonian flow or a weak structural viscosity. It has been found that the fiber drawing is easiest for the sols which are typically Newtonian.

KEY WORDS: Sol-gel/ Flow property/ Alumina/ Fibers/ Viscosity/ Fiber drawing/

I. INTRODUCTION

In the previous study [1] [2] on the alumina fiber formation by unidirectional freezing of gel, it has been pointed out that the gel should be free from anions to obtain continuous fibers. In our study [3] on the sol-gel fiber formation from inorganic alumina sols, however, it has been confirmed that the presence of Cl^- ion does not disturb, rather helps the fiber drawing from the viscous sol, when the sol contains one-dimensionally developed, long-shaped particles. It has been also found that the sols containing round-shaped particles do not have a spinnability and so fibers can not be drawn even if it become viscous [3].

In the present study, the effects of the contents of Al_2O_3 component and Cl^- ions on the flow property of the sol and microstructure of the sol have been examined and these have been related to the fiber drawing behavior of the sol.

II. EXPERIMENTAL PROCEDURES

2.1 Preparation of sol

Table 1 shows the characterization of sols used in this study. All the sols were prepared by heating a 200 cm^3 suspension in reflux at about 100°C for 18 hours. The starting suspension was prepared by adding 5.0 mol (sol 1), 3.8 mol (sol 2) or 3.0 mol (sol 3) Al powders to 1.0 mol/dm^3 $\text{AlCl}_3 \cdot 6\text{H}_2\text{O}$ [4] [5]. For sol 4, 0.06 ml 36% HCl was added to 1.0 mol/dm^3 $\text{AlCl}_3 \cdot 6\text{H}_2\text{O}$ solution. Starting suspensions for sols 5, 6 and 7 were prepared by removing 0.8 mol/dm^3 , 1.3 mol/dm^3 and 1.5 mol/dm^3 of Cl^- ions respectively, from 1.0 mol/dm^3 $\text{AlCl}_3 \cdot 6\text{H}_2\text{O}$ solution with anion exchange resins under a monitor of pH. Sol 8 was prepared by heating the solution in which about 1 mol/dm^3 of Cl^- ion was exchanged with with CH_3COO^- ion. The Al_2O_3 content of sols 4-8 was kept constant at 2.4 mol/dm^3 . The Cl^- ion content of the solutions and sols were measured with a Cl^- ion electrode.

* 牧 俊夫, 作花 清夫: Laboratory of Ceramic Chemistry, Institute for Chemical Research, Kyoto University, Uji, Kyoto-Fu 611.

Table 1. Characteristics of alumina sols used in this study

Sol	Appearance	Al ₂ O ₃ content (mol/dm ³)	Cl ⁻ ion content (mol/dm ³)	Initial pH	Viscosity* at 25°C (poise)	Gelation time at 60°C (h)	Shape of particles
1	Transparent	3.0	2.0	3.8	0.12	80	linear
2	Transparent	2.4	2.0	3.2	0.035	125	linear
3	Transparent	1.9	2.1	3.0	0.030	150	linear
4	Transparent	2.4	3.0	3.1	0.034	135	linear
5	Transparent	2.4	1.2	3.6	0.033	140	linear
6	Transparent	2.4	0.7	4.1	0.033	150	linear
7	Opaque	2.4	0.5	4.3	0.200	15	linear granular
8	Transparent	2.4	0.9	3.8	0.035	100	linear

(+CH₃COO⁻ 1.1)

† All sols were prepared by heating the solution at about 100°C in reflux. The solutions were prepared by dispersing AlCl₃·6H₂O and Al powders in water in given amounts.

* Viscosity of the starting sol measured with an Ostwald viscometer.

2.2 Gelation

30 cm³ of the sol was put into plastic vessels of 80 cm³ capacity and gelled in an oven at 60°C. The lid of the vessels was perforated with nine holes of 2 mm in diameter to promote gelation. The weight loss due to vaporization of the solvent was recorded. All sols gelled in 3-7 days as shown in Table 1.

2.3 Electron microscopy, DTA and infrared measurement

The shape of particles found in the sols was examined by a transmission electron microscope. The sol samples were freeze-dried. The whole picture of sols including the particles was observed by an optical microscope with transparent pieces found in freeze-dried samples [6] [7].

DTA and IR measurements were made with freeze-dried samples. KBr method was used for the latter measurement.

2.4 Measurement of flow properties

The viscosity of a sol as a function of aging time and the change of viscosity with the shear rate were measured with a cone and plate type rotational viscometer at 25°C. The latter measurement was made by increasing and decreasing the rotational rate of the viscometer.

III. RESULTS

3.1 Effect of Al₂O₃ content on morphology of sol particles

Figure 1 shows the TEM pictures of particles found in sols 1, 2 and 3. Fig. 1 (a) shows the pictures of particles in as-prepared sols (starting sols). Fig. 1 (b) shows those of particles in the sols after their viscosity reached about 100 poise as a result of growth of particles or increase of particle density. It is seen that the particles are fibrous and the diameter of the fibers decreases as the Al₂O₃ content of the sol decreases. It is also seen that the particles in

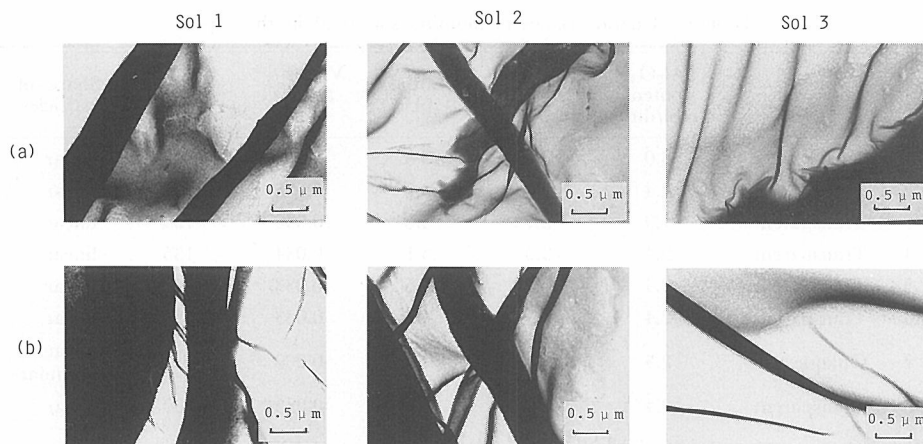


Fig. 1. Transmission electron micrographs of particles found in alumina sols. (a) starting sols, (b) sols whose viscosity is about 100 poise. Al_2O_3 concentrations are 3.0 in sol 1, 2.4 in sol 2 and 1.9 mol/dm^3 in sol 3, respectively.

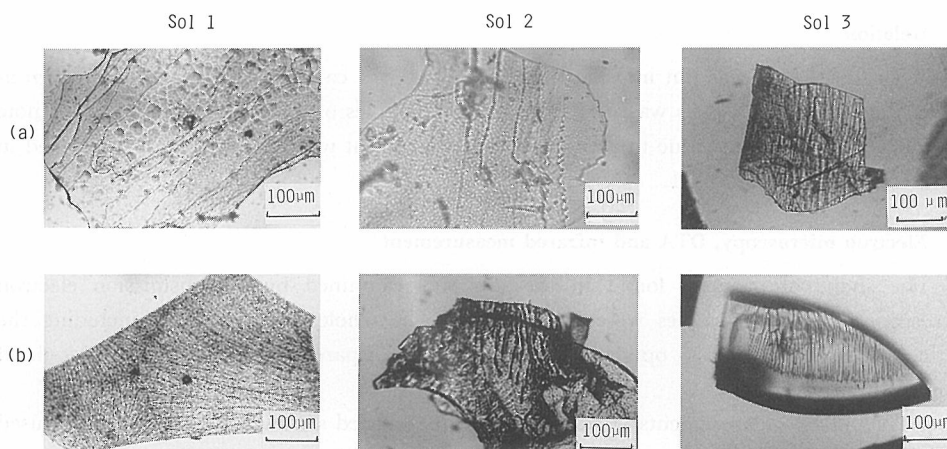


Fig. 2. Optical micrographs of freeze-dried alumina sols. (a) starting sols, (b) sols whose viscosity is about 100 poise. Al_2O_3 concentrations are 3.0 in sol 1, 2.4 in sol 2 and 1.9 mol/dm^3 in sol 3, respectively.

sols 1 and 2 have a wide distribution in length and diameter.

Figure 2 shows the optical microphotographs of the freeze-dried samples of the starting sols (a) and the sols whose viscosity reached about 100 poise (b), respectively. It is seen that particles line up with relatively wide interspaces in the starting sols and at narrow interspaces in the viscous sols (sols 1, 2 and 3).

3.2 Effect of Al_2O_3 content on flow properties

Figure 3 shows the viscosity versus aging time curves for sols 1, 2 and 3. It is seen that as the Al_2O_3 content in sols decreases, the viscosity at start decreases and the gelling time increases. Figure 4 (a), (b) and (c) show the viscosity change of sols 1, 2 and 3, respectively, as a function of the shear rate. It is seen that the sol of 3.0 mol/dm^3 Al_2O_3 content shows weak

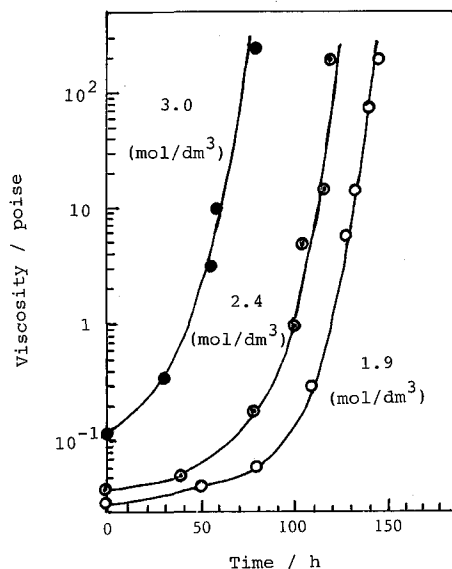


Fig. 3. Viscosity change as a function of aging time for sol 1(Al_2O_3 , 3.0), sol 2(Al_2O_3 , 2.4) and sol 3(Al_2O_3 , 1.9 mol/dm^3), respectively.

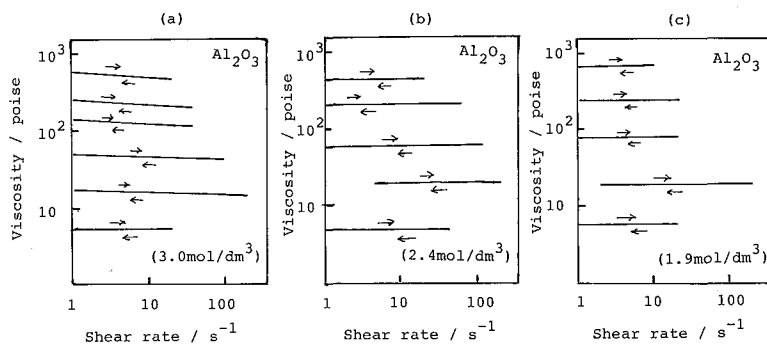


Fig. 4. Plots of viscosity versus shear rate for sol 1(a), sol 2(b), sol 3(c). Arrows show the direction of the change of shear rate.

structural viscosity at viscosities higher than 10 poise and the sols of 2.4 mol/dm^3 and 1.9 mol/dm^3 Al_2O_3 content show Newtonian flow throughout the viscosity range in which measurements were made.

3.3 Effect of Cl^- ion content on morphology of sol particles

Figure 5 shows the TEM pictures of particles found in starting sols and the sols whose viscosity reached about 100 poise for sols 4, 5 and 6. It is seen that long-shaped particles approach mutually and thin, linear and granular particles appear as the Cl^- ion content decreases. Figure 6 shows the optical micrographs of freeze-dried sols 4, 5 and 6. It is seen that for the sol rich in the Cl^- ion the interspaces of long-shaped particles are narrow, and that the interspaces in starting sols as well as in viscous sols become narrow as the Cl^- ions decrease.

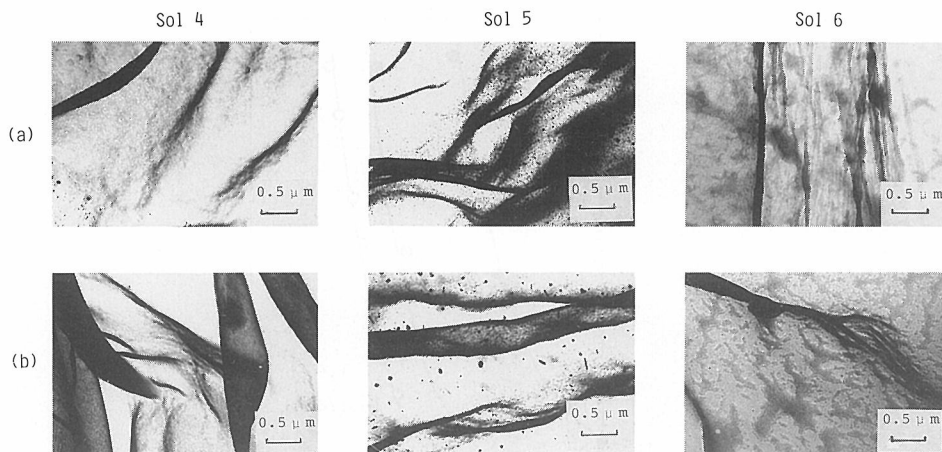


Fig. 5. Transmission electron micrographs of particles found in alumina hydrous sols. (a) starting sols, (b) sols whose viscosity is about 100 poise. Cl^- ion concentrations are 3.0 in sol 4, 1.2 in sol 5 and 0.7 mol/dm³ in sol 6, respectively.

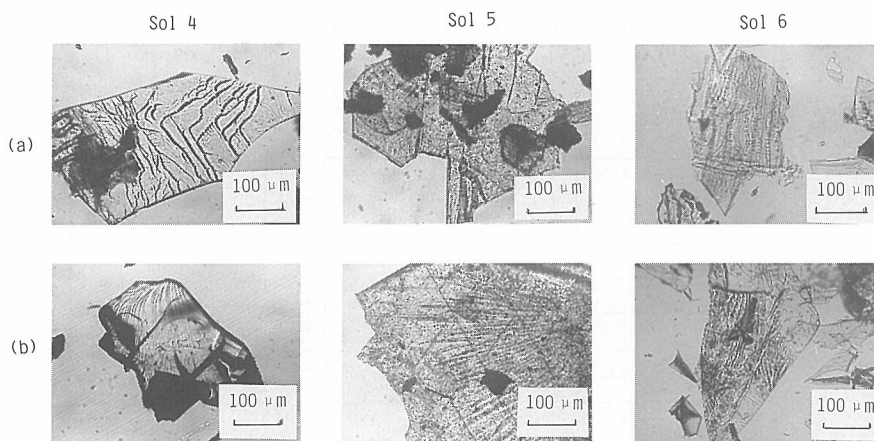


Fig. 6. Optical micrographs of freeze-dried alumina sols. (a) starting sols, (b) sols whose viscosity is about 100 poise. Cl^- ion concentrations are 3.0 in sol 4, 1.2 in sol 5 and 0.7 mol/dm³ in sol 6, respectively.

3.4 Effect of Cl^- ion content on flow properties

Figure 7 shows the viscosity versus aging time curves for sols 4, 5 and 6. It is seen that the viscosity of the sol with 2.0 mol/dm³ Cl^- ion content is the largest among the three. The dotted curve in the figure shows the viscosity increase in the sol in which about a half of 2.0 mol/dm³ Cl^- ions was exchanged with the CH_3COO^- ions. In this case, the viscosity increase is quicker than that of the sol of 2.0 mol/dm³ Cl^- ions.

In a separate experiment, it was tried to prepare a sol using the solution in which a half of Cl^- ions was exchanged with SO_4^{2-} ion, but no uniform sol could be prepared because of precipitation of particles.

Figure 8 (a)–(b) show the viscosities of sols 4–7, respectively, as a function of the shear rate. It is seen that slight structural viscosity develops as the Cl^- ion content decreases and

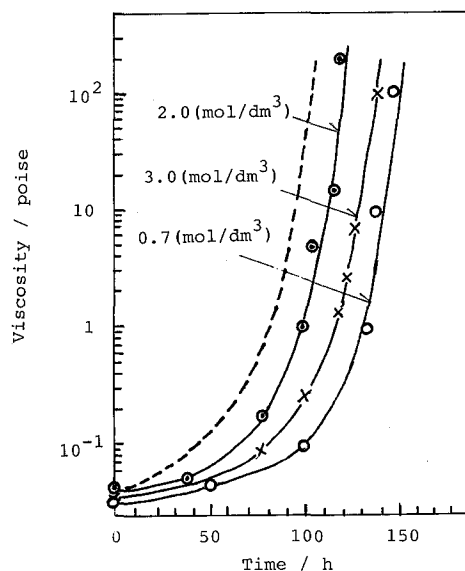


Fig. 7. Viscosity change as a function of aging time for sol 2(Cl^- , 2.0), sol 4(Cl^- , 3.0) and sol 6(Cl^- , 0.7 mol/dm³). A dotted line shows the viscosity curve for sol 8 in which the Cl^- ion have been partly exchanged with CH_3COO^- ions. Viscosity was measured at shear rate of $2/\text{s}^{-1}$. Aging was carried out at 60°C .

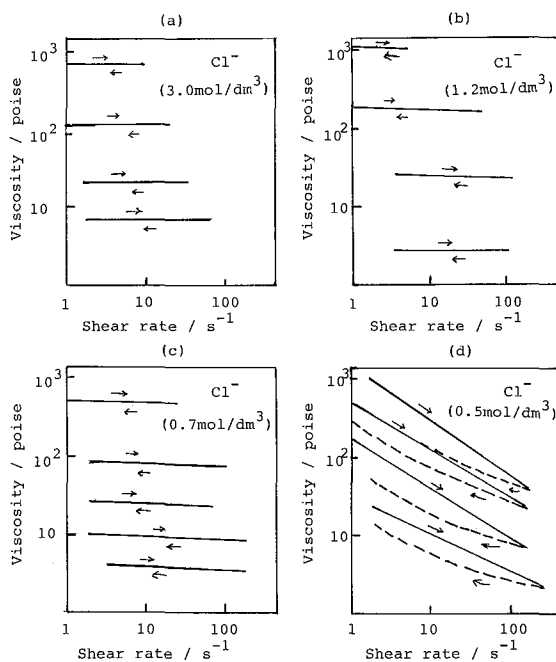


Fig. 8. Plots of viscosity versus shear rate for sol 4(a), sol 5(b), sol 6(c) and sol 7(d). Arrows show the direction of the change of shear rate.

when the content is 0.5 mol/dm³, the structural viscosity becomes large and accompanied with thixotropy.

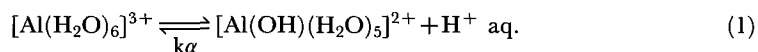
3.5 Effect of Al₂O₃ and Cl⁻ contents on fiber formation

Thick long fibers of 50 - 100 μm in diameter but not thinner fibers could be drawn from the sol of 3.0 mol/dm³ Al₂O₃ content. The drawing of thin long fibers of 10 μm in diameter was possible with the sol of 2.4 mol/dm³ Al₂O₃ content. This difference might be caused by the difference of flow properties, that is, structural or Newtonian flow at higher viscosities than about 10 poise. When the Cl⁻ ion content decreased to 0.7 mol/dm³, the fiber drawing became difficult regardless of the fiber diameter.

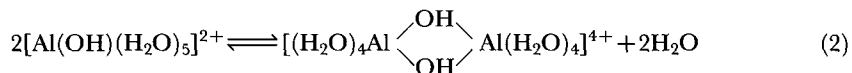
IV. DISCUSSION

1. Formation of sol

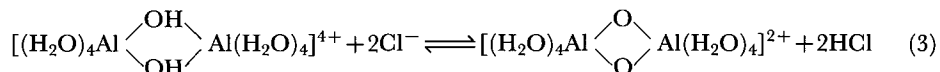
The formation of long-shaped particles can be discussed on the basis of the concept of Baes and Mesmer [8]. It is assumed that hydrolysis takes place in equation (1).



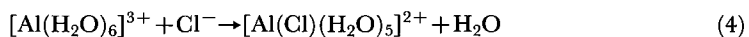
Here $K\alpha$ is a dissociation constant. Simultaneously, polymerization of hydrous alumina species may be initiated by the reaction expressed in equation (2).



In the solution of high Cl/Al ratio, the Cl⁻ ions promote the formation of oxo bridge as shown by equation (3)



The connection of either or both of these aluminous complexes might lead to formation of various sizes of linear particles, depending on the Al₂O₃ and Cl⁻ ion contents. Some of the Cl⁻ ions may perhaps be incorporated into the aluminous complexes as shown in equation (4).



The formation of this complex would give a large influence on the properties of particles in sols. When the sol thus obtained are kept in the vessel at 60°C, the linear particles increase to some extent in size and in number in the gelation process. It is assumed from microphotographs that the linear aluminous particles have a tendency to line up parallel at interspaces in a direction horizontal to the base of the vessel as the solvent vaporizes from the sol. This would mean that similar lining up may take place on fiber drawing from sols.

2. Effect of Al₂O₃ content on gelation time

Figure 9 shows the viscosity change of sols at viscosities over 0.1 poise as a function of Al₂O₃ content of sols. It is interesting to see that the sol of 1.9 mol/dm³ Al₂O₃ content shows

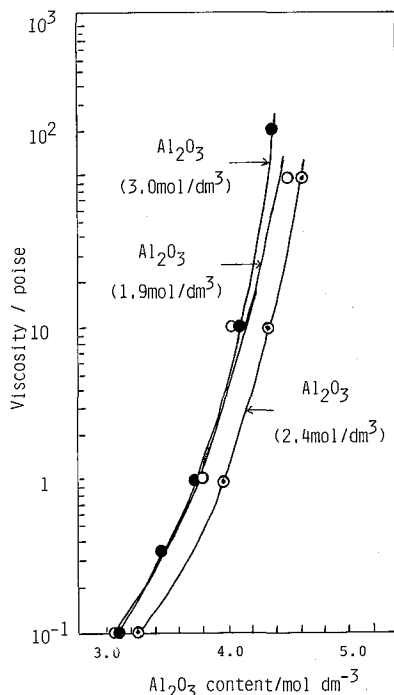


Fig. 9. Viscosity change as a function of Al_2O_3 content for sols 1, 2 and 3. The figure was induced from Fig. 3 and decrease in volume of sol during aging.

the same viscosity as that of the sol of 3.0 mol/dm^3 Al_2O_3 content at the same Al_2O_3 content. This means that the long shaped particles in the sols of 3.0 and 1.9 mol/dm^3 Al_2O_3 contents are similar in number and slightly different from that of 2.4 mol/dm^3 Al_2O_3 content. In the sol of 1.9 mol/dm^3 content, the contact between sol particles is assumed to take place in lower Al_2O_3 content than that in the sol of 2.4 mol/dm^3 content as a result of evaporation of solvent.

3. Effect of Al_2O_3 content on flow properties

As seen from the photographs of freeze-dried sols whose viscosity is about 100 poise, in the sols of 2.4 and 1.9 mol/dm^3 , linear particles line up without mutual contact (Fig. 2 (b)). It is attributed to the linear particles lining up at interspaces that the flow of these sols shows Newtonian at viscosities higher than about 10 poise. In the sol of 3.0 mol/dm^3 , the linear particles contacting each other line up in the sol of 100 poise (Fig. 2 (b)). The small structural viscosity is considered to develop by this contact. The degree of structural viscosity expressed by the slope of the straight line is constant in the range of 10–1000 poise. This is probably caused by the fact that the nature of bonding does not change greatly throughout this viscosity range, although straight particles but also spiral and bending particles are observed in Fig. 2 and 10.

4. Effect of Cl^- ion content on gelation time

The Cl^- ion contents in as-prepared sols 1, 2 and 3 are nearly the same, i.e., 2.0 mol/dm^3 (Table 1). Since the Cl^- ion content of the starting solution is 3.0 mol/dm^3 , the rest of Cl^-

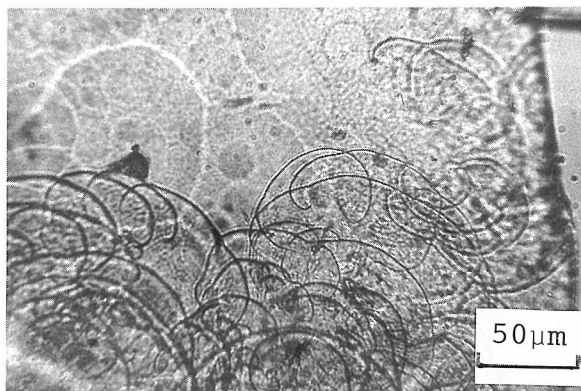


Fig. 10. Optical micrograph of linear bending particles found in freeze-dried sample of sol 1 (Al_2O_3 content, 3.0 mol/dm^3).

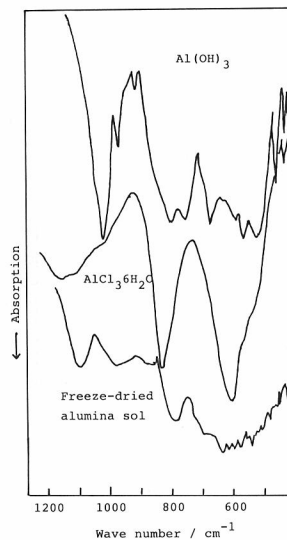


Fig. 11. IR spectrum of freeze-dried sample (sol 1, 2 or 3).

ions (1 mol/dm^3) must have been incorporated into the Al_2O_3 hydrous particles. The IR spectrum of freeze-dried sample of the sol mentioned above shows a spectrum similar to that of $\text{Al}(\text{OH})_3$ or $\text{AlCl}_3 \cdot 6\text{H}_2\text{O}$ as seen in Fig. 11. The presence of Cl^- ions in aluminous hydrates is also shown by the fact that the precipitation took place at lower pH value than the isoelectric point of pure aluminous hydrates particles [9].

The Cl^- ions incorporated in particles will affect the electric charge of long-shaped Al_2O_3 particles. In the sol with 3.0 mol/dm^3 in the Cl^- ion content, the alumina hydrous particles attract H^+ ions rather than Cl^- ions in the electric double layer, causing the higher net positive charge of particles than that in the sol of 2.0 mol/dm^3 in the Cl^- ion content [10]. This may be the reason for slower viscosity increase of the sol with 3.0 mol/dm^3 Cl^- ion content.

On the other hand, in the sol of 0.7 Cl^- ion content, the Cl^- ions present between the Al_2O_3 particles are not sufficient, and so the repulsing force between the particles may be larger than that in the sol of 2.0 mol/dm^3 Cl^- ion. This would cause the slower viscosity increase than that of the sol with 2.0 mol/dm^3 in the Cl^- ion content. The exchange of the Cl^- ions with CH_3COO^- ions in the sol results in an increase of the pH of the sol, decreasing the net positive charge surrounding the particles. This would cause the quicker viscosity increase than that of the sol of 2.0 mol/dm^3 in the Cl^- ion content.

5. Effect of Cl^- ion content on flow properties

As the Cl^- ion content decreases from 3.0 to 1.0 mol/dm^3 , the flow behavior changes from Newtonian to weak structural viscosity at higher viscosities than about 10 poise. Similar behavior is seen in the sol of 0.7 mol/dm^3 Cl^- ion content at lower viscosities than 10 poise (Fig. 8 (a), (b) and (c)). This reason becomes clear from the photographs of freeze-dried sol showing that the interspaces between linear particles are narrow in starting sols as well as in viscous sols whose viscosity is 100 poise (Fig. 6). When the Cl^- ion content decrease further

down to 0.7 mol/dm^3 a large structural viscosity and a thixotropy appear. This phenomenon is attributed to the structure of particles in sols, which have grown to long and thick particles due to an increase of pH of the sol, causing interlocking and including a large amount of water in the interstice.

REFERENCES

- (1) T. Maki, T. Kokubo and S. Sakka, *Bull. Inst. Chem. Res., Kyoto Univ.*, **64**, 292 (1986).
- (2) T. Maki and S. Sakka, *J. Mater. Sci. Lett.*, **5**, 28 (1986).
- (3) T. Maki and S. Sakka, *J. Non-Cryst. Solid*, in press.
- (4) J. Bugosh, *J. Phys. Chem.*, **65**, 1789 (1961).
- (5) J. Bugosh, et al., U. S. Patent 2, 915, 475 (1959).
- (6) F. Schnetter et al., "Science of Ceramics" **4**, 79 (1968).
- (7) T. Mihara, *Seramikkusu*, **16**, 848 (1981).
- (8) C. Baes, Jr. and R. Mesmer, "The Hydrolysis of Cations" John Wiley & Sons, 1976, p.112.
- (9) G. Parks, *Chem. Rev.*, **65**, 177 (1965).
- (10) G. Onoda, Jr. and J. Casey, "Ultrastructure Processing of Ceramics, Glasses, and Composites, L. Hench & D. Ulrich eds., John Wiley & Sons, 1984, p. 374.